Computer Aided Surgery 7:146–155 (2002)

Biomedical Paper

Registration of 3D CT and Ultrasound Datasets of the Spine using Bone Structures

B. Brendel, Dipl. Ing., S. Winter, A. Rick, Ph.D., M. Stockheim, M.D., and H. Ermert, Ph.D.
Institute of High Frequency Engineering (B.B., H.E.), Institute of Neuroinformatics (S.W.), and Department of Orthopedic Surgery (M.S.), Ruhr-University Bochum, and ZN Vision Technologies AG (A.R.), Bochum, Germany

ABSTRACT

Objective: In navigated orthopedic surgery, accurate registration of bones is of major interest. Usually, this registration is performed using landmarks positioned directly on the bone surface. These landmarks must be exposed during surgery. Our goal is to avoid the exposure of bone surface for the sole purpose of registration by using an intraoperative ultrasound device that can localize the bone through tissue.

Method: We propose an algorithm for the registration of CT and ultrasound datasets that takes into account the fact that ultrasound produces very noisy images (speckle) and shows only parts of the bone surface. This part is made from the CT dataset. Next, a surface volume registration is performed by searching for a position of the estimated surface that maximizes the average gray value of the voxels in the ultrasound dataset covered by the surface.

Results: The algorithm was implemented and validated using an ex vivo preparation of a human lumbar spine with surrounding muscle tissue. On the basis of this data, the method has a large radius of convergence and a repeatability of 0.5 mm for displacement and 0.5 degrees for rotation.

Conclusions: A robust algorithm for the registration of 3D CT and ultrasound datasets is presented. The computation time seems sufficiently short to permit intraoperative use. Comp Aid Surg 7:146–155 (2002). ©2002 Wiley-Liss, Inc.

Key words: **registration; intraoperative imaging; ultrasound; spine; orthopedic surgery**

INTRODUCTION

An important prerequisite of minimally invasive computer-assisted surgery is the precise registration of preoperative datasets (mostly CT or MRI) within the coordinate system of the navigation system. In the case of orthopedic surgery, the main interest lies in accurate registration of bones.

Registration Methods

For the registration of two coordinate systems, identical points in both systems must be associated. Many different methods exist for the registration of preoperative images and the patient coordinate system during surgery.[1–3] The majority of these methods are based on landmarks, which can be anatomical landmarks or fiducial markers. The accuracy of these registration methods depends on the number of points and on the ability of these points to move with respect to the structure of interest (in this case, the bones).[4,5] For a precise registration, a large number of anatomical landmarks on the bone sur-

Received May 5, 2002; accepted July 7, 2002.

Address correspondence/reprint requests to: Bernhard Brendel, Ruhr-University Bochum, IC6/140, 44780 Bochum, Germany. E-mail: bernhard.brendel@ruhr-uni-bochum.de

Published online in Wiley InterScience (www.interscience.wiley.com). DOI: 10.1002/igs.10038

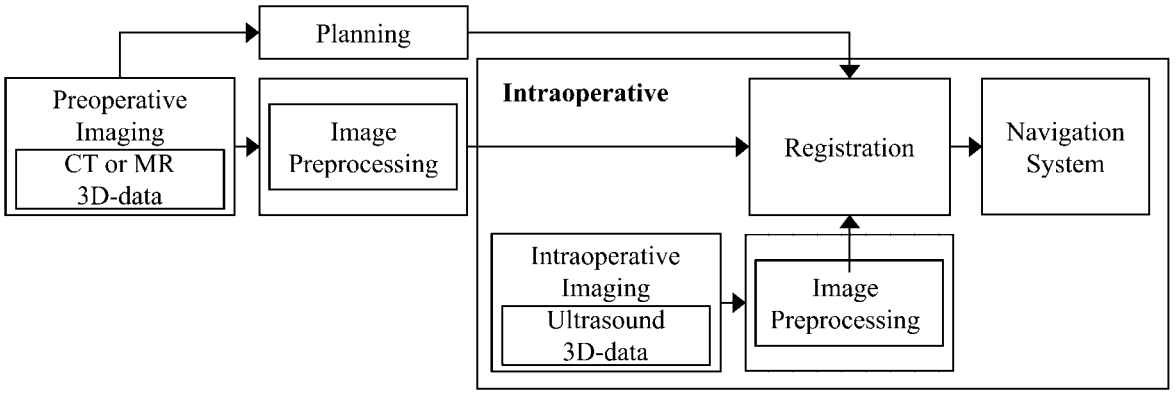

Fig. 1. Structure of a navigated surgical procedure with intraoperative imaging.

face must be used and consequently tagged in the CT dataset. Intraoperatively, all these points must be referenced with the pointing device of the navigation system. Alternatively, a few fiducial markers (usually screws) can be used. These are fixed to the bone preoperatively to ensure high precision for the registration.

These procedures are time consuming and increase invasiveness, because the fiducial markers are connected to the bone and anatomical landmarks are exposed during surgery. Furthermore, changes in the anatomy during the surgical procedure cannot be visualized.

To avoid these disadvantages, intraoperative imaging modalities are used. In this case, complete anatomical structures can be used for registration (mostly surfaces[6]), thus increasing the accuracy. Intraoperative changes in the anatomy can also be taken into consideration. A few CT- or MRI-based systems have already been implemented,[7,8] but these have major disadvantages with respect to cost, application difficulties, and radiation exposure (in CT-based systems). In view of these drawbacks, intraoperative ultrasound could be a solution,[9–13] offering the advantages of fast, inexpensive, and easy data acquisition. Furthermore, in contrast to intraoperative CT or MRI systems, ultrasound machines occupy only a little space in the operating room.

Intraoperative Ultrasound

The concept of intraoperative ultrasound is shown in Figure 1. As in conventional navigation procedures, preoperative datasets are acquired and used for planning and intraoperative visualization. Additionally, these datasets are preprocessed to accelerate the intraoperative registration. Because this preprocessing can be done prior to surgery, the algorithms are not time-critical.

During the surgical procedure, ultrasound data is acquired with a transducer that is tracked by the navigation system and has been calibrated to determine the coordinate system of the imaging plane.[14–16] Then, the acquired images are combined into a 3D dataset that is used for registration. Because ultrasound can easily be applied intraoperatively, the registration can be repeated several times during the procedure to take into account movements of bones relative to each other. This is of particular interest in spinal procedures.

Bone Surface Imaging with Ultrasound

The major problem of intraoperative ultrasound is its low imaging quality; the acquired data is very noisy due to speckle. In addition, ultrasound images show only a small part of the bone surface, due to the reflection properties of an ultrasound beam at the tissue–bone interface.[17]

The two main consequences of these reflection properties are shown in Figure 2. Because there is a great difference in the acoustic impedances of tissue and bone, almost the entire ultrasound wave is reflected at the interface, so no imaging is possible beyond it (Fig. 2, left). Furthermore, the reflection is almost completely specular. Because of this, interfaces that are not orthogonal to the direction of sound propagation deliver a weak image or no image at all (Fig. 2, right). For these two reasons, only a small part of the bone surfaces can be visualized with ultrasound. This is illustrated in Figure 3 using the example of a lumbar vertebra. The direction of ultrasound propagation is expected to be from posterior to anterior. Structures accessible for ultrasound image acquisi-

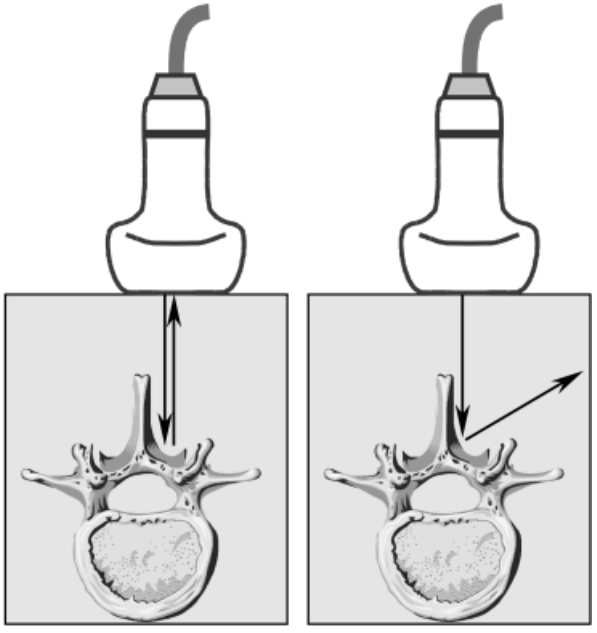

Fig. 2. Left: total reflection of the ultrasound wave at the tissue–bone interface inhibits imaging of the vertebral body, because it is covered by the posterior elements of the vertebra. Right: specular reflection of the ultrasound wave at the tissue–bone interface inhibits imaging of the right surface of the spinous process, because the ultrasound wave is not reflected towards the transducer.

tion include the transverse processes, the lamina, the inferior articular facets, and the posterior edge of the spinous process. The vertebral body, the pedicles, and the superior articular facets are covered by elements of the vertebra in the posterior direction, and thus cannot be imaged. The left and right surfaces of the spinous process cannot be seen because of their disadvantageous orientation with respect to the ultrasound propagation.

Fig. 3. Model of a lumbar vertebra. The surfaces of the bone that can be visualized with ultrasound are marked in gray.

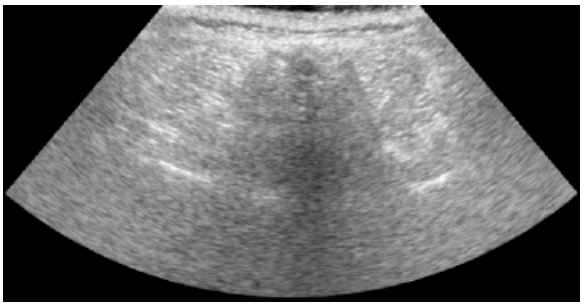

Fig. 4. Typical ultrasound image of a lumbar vertebra (cranial view) recorded with a 3.5-MHz curved array. In this plane, only the spinous process and the transverse processes are visible.

A typical ultrasound image of a lumbar vertebra is shown in Figure 4. A navigated surgery would be impossible based on this data alone, so preoperative data is also needed. In the following section, it is assumed that a 3D CT dataset has been acquired preoperatively.

METHODS

An algorithm for the registration of 3D CT and ultrasound datasets must take into account the problems and restrictions of ultrasound imaging. A segmentation of bone surfaces in the ultrasound dataset seems to be difficult to implement in a robust way, considering the quality of the images (see Fig. 4). Therefore, as a first step, we propose an estimation of the surface that is expected to be visible in the ultrasound images, based on the CT data.

Surface Estimation

As mentioned above, the visibility of bone surfaces depends on the direction of ultrasound propagation. Therefore, the surgeon should preoperatively indicate in the CT dataset the way in which he wants to move the transducer. An example of this, applied to the lumbar spine, is given in Figure 5, where the skin is visualized as being semitransparent so that the underlying bones can be seen. The line marks the scanning path of the transducer. It is assumed that the imaging plane is approximately orthogonal to the skin surface and the scanning path, so a reasonable volume dataset can be recorded. With

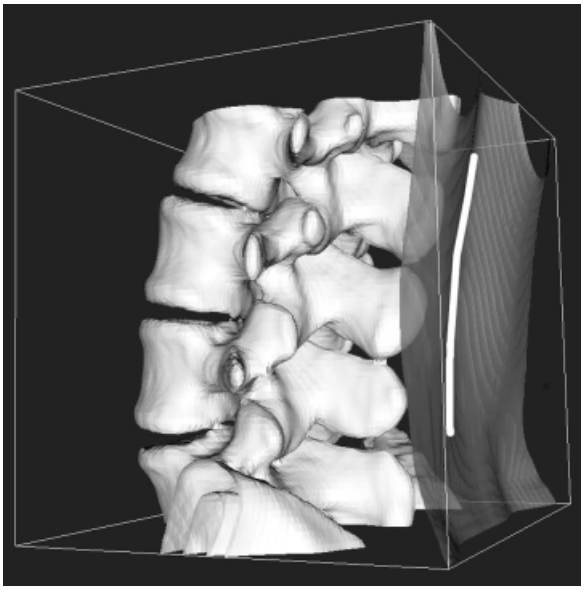

Fig. 5. Bone surface of the lumbar spine and skin surface extracted from a CT dataset. The white line marks the planned scanning path of the ultrasound transducer.

the knowledge of the scanning path and the transducer geometry, it is possible to estimate a bone surface in the CT dataset that would be visible in a corresponding ultrasound dataset.

The estimation procedure is illustrated in Figure 6, again showing the example of the lumbar spine. First, the complete bone surface is determined by simple thresholding in the CT dataset (Fig. 6, left). Then, each element of the surface is tested for its visibility to the transducer, i.e., to see if there is any other surface element between it and the transducer. This visibility check takes into consideration the complete reflection of the ultrasound wave at the first tissue–bone interface. These parts of the surface can be seen in the middle image of Figure 6. In the next step, the angles between the normal vectors of the visible surface elements and the direction of ultrasound propagation are calculated. If some of these angles exceed a defined threshold, it is assumed that the associated surface elements cannot be imaged because of the specular reflection of the ultrasound wave. Thus, the resulting surface (shown in Fig. 6, right) takes into account both restrictions on bone surface visualization with ultrasound (see Figs. 2 and 3).

The bone surface is the only anatomical structure that can be used for precise registration of a bone, because all other anatomical structures can move relative to it. Thus, the estimated surface should provide enough input information for the registration algorithm from the CT dataset.

Registration

As mentioned above, a robust segmentation of the ultrasound dataset would be very difficult and, for a whole 3D dataset, very time consuming. Therefore, the best way to achieve registration seems to be a surface–volume registration, which tries to find the correct position of the estimated surface in the ultrasound dataset.

First, a criterion must be defined that gives evidence of the correctness of the chosen position of the estimated surface in the ultrasound dataset. Because the tissue–bone interface is imaged as a bright curve with ultrasound because of the total reflection, a suitable local criterion is the average gray value of all voxels that are covered by the surface. This criterion has the advantage that the averaging of a large number of voxels eliminates the noisy character of the ultrasound data. Further-

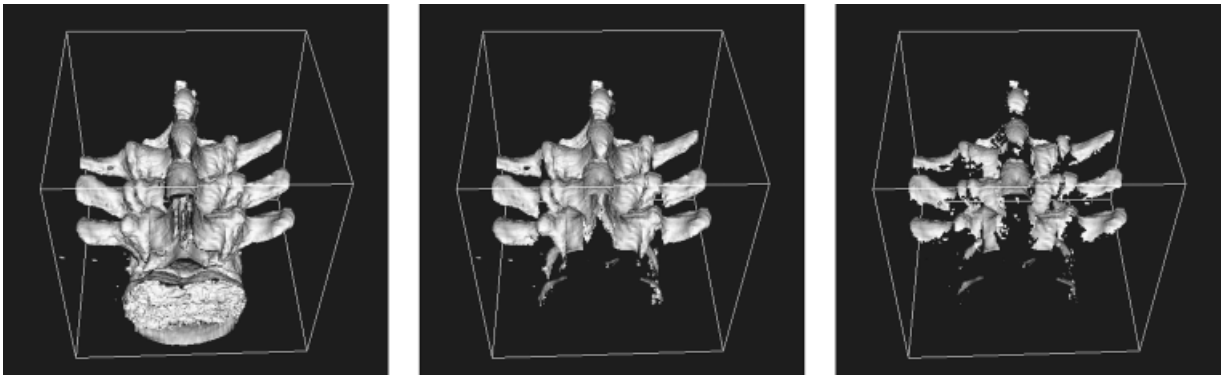

Fig. 6. Left: Bone surface of the lumbar spine. Center: Part of the bone surface that can be reached with the ultrasound wave. Right: Part of the bone surface that can be imaged with ultrasound.

more, the complete surface is evaluated in the criterion, avoiding disturbing influences of other bright structures with different shapes. It is assumed that the average gray value is maximal at the correct position of the surface. This is generally true, due to the unique surface of the vertebra when seen from the posterior. The only ambiguity that may arise when just a small section of the spine is visualized is a translation along the spine axis of one vertebra due to the similarity of the adjacent vertebrae.

For an effective realization of a registration algorithm based on this average gray value, the surface should be described in such a way that the gray values of the corresponding locations in the ultrasound dataset can easily be determined. This is true for a surface that is represented only by the center coordinates of the surface elements. Thus, the surface consists of N points $\vec{p}_i = (x_i,y_i,z_i), \quad i = 1 \ldots N$. A simple and fast nearest-neighbor interpolation is used to determine the gray value of the corresponding locations in the ultrasound data. The average gray value $\bar{g}$ can then be written as follows:

$$\bar{g}(\alpha,\beta,\gamma,\vec{g}) = \frac{1}{N} \sum_{i=1}^{N} UV(\mathbf{A}(\alpha,\beta,\gamma) \cdot \vec{p}_i + \vec{q})$$

where $\mathbf{A}$ (α, β, γ) is the rotation matrix, which depends on the three angles α, β, and γ. $\vec{q}$ is the translation vector, and $UV(\vec{p})$ delivers the gray value at the location $\vec{p}$ in the ultrasound data with nearest-neighbor interpolation. The registration procedure can be formulated as an optimization problem: α, β, γ, and $\vec{q}$ are the parameters that must be optimized to find the maximum of the average gray value $\bar{g}$. The resulting values of the parameters describe how the CT dataset must be transformed to fit with the ultrasound dataset. The maximization can be performed with any of the classical optimization algorithms, such as gradient descent, the simplex rule, or the Levenberg-Marquart method. Due to the smoothness of the optimization function, a very simple local deepest-descent method is sufficient for small misalignments of the two datasets. The initialization can be based on the ultrasound scanning path indicated on the preoperative dataset.

EXPERIMENTS AND RESULTS

The described registration algorithm was implemented and evaluated using CT and ultrasound datasets acquired from an ex vivo preparation of a human lumbar spine with surrounding muscle tissue.

Data Acquisition

CT data was acquired using a spiral CT scanner. The table speed was 6 mm/s, the slice thickness 3 mm, the reconstruction interval 2 mm, the gantry angle 0°, and the scanning direction craniocaudal. The field of view was set to 200 × 200 mm^2, resulting in an in-plane resolution of 0.39 × 0.39 mm^2. The whole lumbar spine was scanned in this way.

The 3D ultrasound data was acquired with a 3.5-MHz curved array. The transducer was moved mechanically in the craniocaudal direction with a transverse imaging plane (roughly equivalent to Fig. 5). B-scans were acquired at a craniocaudal distance of 1 mm. With ultrasound imaging, the slice thickness and in-plane resolution are anisotropic and depth dependent. Again, the whole lumbar spine was recorded.

Both datasets were resampled to obtain an isotropic voxel resolution of 0.5 mm, and the resulting 3D volumes were used for the registration algorithm.

Result of Surface Estimation

The first step was the surface estimation based on the CT data. The estimated surface comprised 60,000 elements for the given data of the lumbar spine. An example of an estimated surface and the corresponding ultrasound image are shown in Figure 7. The left image of Figure 7 shows a CT slice of a lumbar vertebra with the estimated surface plotted as a black curve. The estimation process delivers a result that matches the visibility prediction for the surface of a vertebra in Figure 3. The middle image of Figure 7 shows the corresponding ultrasound slice. The tissue–bone interface produces a bright area, and the ultrasound image is dark beyond it. This is due to the total reflection, which inhibits the reception of echoes from deeper structures. Transfer of the estimated surface onto the ultrasound image (Fig. 7, right) shows that the estimation is a very good predictor of the bone surface as visualized with ultrasound.

This surface representation and the acquired ultrasound volume were the input for the registration algorithm. The optimization of the average gray value was initially realized by a deepest descent method.

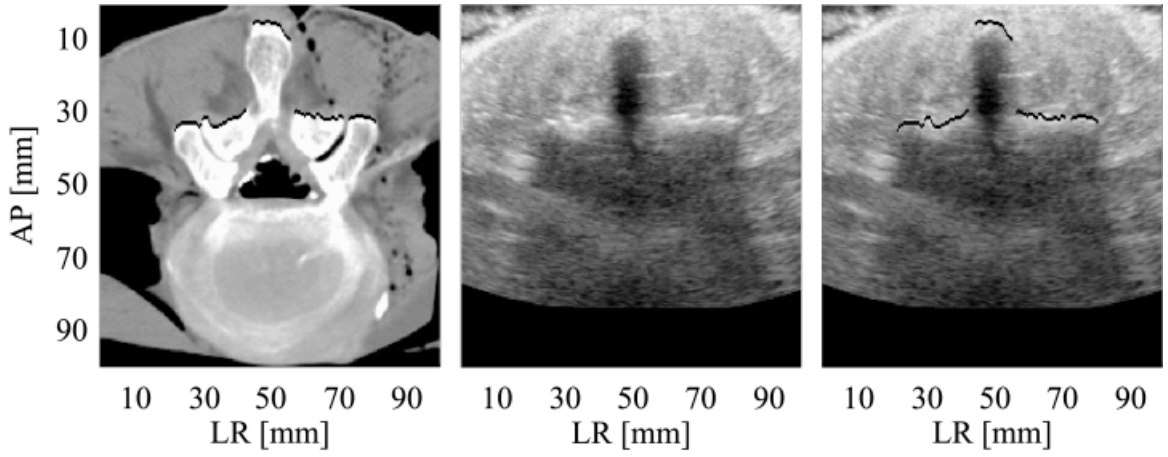

Fig. 7. Left: CT slice of a lumbar vertebra (cranial view). The black line marks the estimated surface. Center: Cranial view of a lumbar vertebra imaged with ultrasound (corresponding to the CT slice). Right: The ultrasound image overlaid with the estimated surface.

Computation Time for Registration

The calculation time for the registration of the whole lumbar spine, assuming that the vertebrae could not move relative to each other, was 50–100 s. For a single vertebra (approximately 7,000 surface elements), the registration took 5–15 s. The computation time depends on the positions of the two datasets before registration. This result was achieved on a 650-MHz processor. Computation time for the surface was excluded, as this can be done preoperatively. The program was realized in Matlab and C, and was not optimized for speed. An example of a registered surface is shown in Figure 8. Based on visual inspection, the algorithm seems to perform correctly, because the match of the estimated surface and the ultrasound image is very good.

Influence of Surface Extraction Parameters

Because the ultrasound data is not preprocessed in this case, the registration result is only affected by the surface estimation. The two main parameters of the surface estimation are the threshold for the extraction of the bone surface in the CT dataset, and the assumed direction of ultrasound propagation. The impact of both these parameters was investigated.

To test the sensitivity of the algorithm with respect to the threshold, this parameter was varied between 100 and 400 Hounsfield units (HU). The registration with 200 HU was deemed to be a reference registration.[18] The maximal deviations of the registration results relative to the reference registration are listed in Table 1. Again, the registration was tested with the complete datasets and with

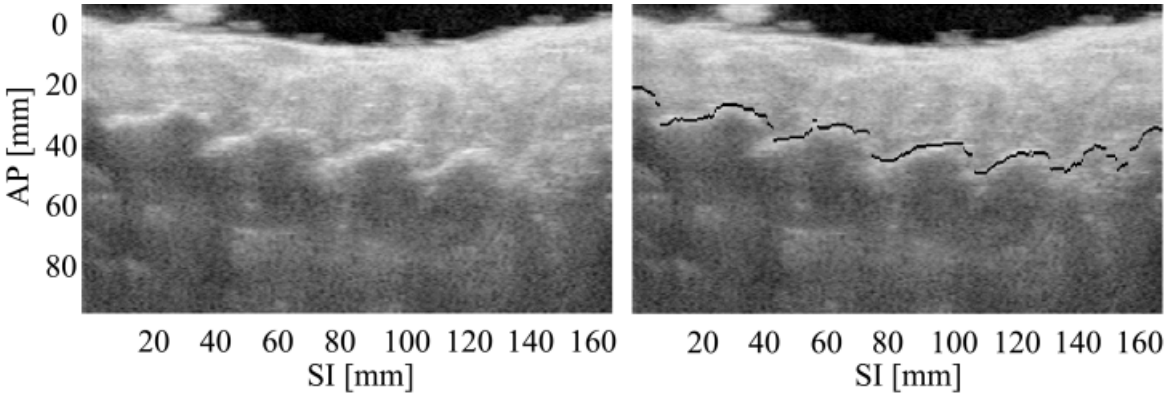

Fig. 8. Left: Reconstructed lateral slice of a lumbar spine imaged with ultrasound. Right: The same image overlaid with the registered estimated surface.

Table 1. Deviation of the Registration Results Depending on the Threshold for the Bone Surface Extraction in the CT Dataset

Threshold	Maximal rotational misalignment (whole spine)	Maximal translational misalignment (whole spine)	Maximal rotational misalignment (single vertebra)	Maximal translational misalignment (single vertebra)
100 HU	0.250°	0.5 mm	0.250°	0.5 mm
200 HU*	0.000°	0.0 mm	0.000°	0.0 mm
300 HU	0.500°	0.5 mm	0.125°	0.5 mm
400 HU	0.375°	0.5 mm	0.625°	0.5 mm

* Reference registration.

a single vertebra. The assumption that the case of the single vertebra would be more critical because of the smaller dimensions was only correct for the 400-HU threshold. Overall, a maximal rotational deviation of 0.625° and a maximal translational deviation of 0.5 mm (which is equal to the resolution) show that the algorithm is not very sensitive with respect to the chosen threshold.

The influence of the assumed direction of ultrasound propagation was checked by varying the angle of incidence within a range of 20 degrees around different axes. Most crucial is an alteration of the angle around the longitudinal axis, because the position of the transducer relative to the spinous process has a great impact on the visibility of the lamina in the ultrasound image. In Table 2, the deviations of registration results from the reference registration are listed for different angle alterations. The reference registration is defined as a registration where the assumed direction of ultrasound propagation for the surface estimation was validated by the registration; i.e., the calculated position of the ultrasound dataset relative to the CT dataset verified the expected angles of incidence. The results (Table 2) show that a difference of 10 degrees between the assumed and real angles of incidence entails an acceptable maximal deviation of 0.5 mm and 0.375°. For larger angle differences, the deviations (up to 1° and 2 mm) seem to be too large. In these cases, a new estimation of the surface must be done to correct the misalignments. Thus, the registration procedure is as follows:

1. A surface is estimated in the CT data, based on the indicated scanning path.
2. Surface and ultrasound data are registered.
3. If the registration implies a difference of more than 10° between assumed and real incidence angles for the ultrasound waves, the surface estimation is rerun based on the direction of ultrasound propagation given by the registration result. The registration is then repeated with the new surface, starting from the last registration position.

Thus, the impact of the assumed incidence angle on the registration result is small and can be corrected. A new intraoperative estimation of the surface increases the computation time substantially, but can be avoided by complying roughly with the indicated scanning path of the transducer. To summarize the results of Tables 1 and 2, the proposed algorithm is very robust with respect to the adjustable parameters of the surface estimation.

Table 2. Deviation of the Registration Results Depending on an Alteration of the Assumed Incidence Angle for the Ultrasound Wave

Alteration of the incidence angle	Maximal rotational misalignment (whole spine)	Maximal translational misalignment (whole spine)	Maximal rotational misalignment (single vertebra)	Maximal translational misalignment (single vertebra)
2°	0.250°	0.5 mm	0.375°	0.5 mm
4°	0.125°	0.5 mm	0.375°	0.5 mm
6°	0.125°	0.5 mm	0.375°	0.5 mm
8°	0.125°	0.5 mm	0.125°	0.5 mm
10°	0.125°	0.5 mm	0.250°	0.5 mm
12°	0.750°	1.5 mm	0.125°	1.0 mm
14°	0.625°	1.5 mm	0.250°	1.0 mm
16°	0.500°	1.5 mm	0.250°	1.0 mm
18°	0.750°	1.5 mm	0.750°	1.5 mm
20°	1.000°	2.0 mm	0.500°	1.5 mm

Radius of Convergence

Another item of interest is the scope of the registration, i.e., the misalignments that can be determined by the algorithm. The optimization with a deepest descent method can lead to wrong registration results due to local maxima. To approximate the scope, the average gray value was determined for different positions of the estimated surface in the ultrasound dataset.

The surface of a single vertebra was rotated around different axes, starting from the registered position. Then, a search was made for the optimal translation for this rotated surface to avoid effects due to the choice of the rotation center. In Figure 9, the maximal average gray values for rotations around the mediolateral axis (solid line), the anterior–posterior axis (dashed line), and the superior–inferior axis (dashed-dotted line) with deviations up to 20° from the registered position are shown. The functions have no further optima with respect to rotations around the mediolateral and anterior–posterior axes. There, the scope of the algorithm is about 20°. A rotation around the longitudinal axis with a deviation of more then 12° cannot be detected correctly by the registration. Nevertheless, the maximum is nonambiguous, and another optimization strategy could find the correct position. Thus, the optimization criterion permits a registration scope for rotational misalignments of at least 20°.

To test the convergence behavior of the algorithm with respect to translational misalignments, the estimated surface of a vertebra was displaced from its registered position in various directions, and the average gray value was calculated. The results can be seen in Figure 10 for a movement in the anterior–posterior (solid line), left–right (dashed line), and superior–inferior (dashed-dotted line) directions. Local maxima appear at displacements of about 30 mm in each direction. Again, these local maxima can mislead a deepest descent method, but a more sophisticated optimization algorithm should have no problem finding the correct optimum. One exception is the local maximum for a 30-mm movement in the posterior direction. This maximum is due to the bright representation of the skin region in the ultrasound images (see Figs. 4, 7). A better-adjusted time-gain compensation (TGC) of the ultrasound machine or an adaptive TGC in the preprocessing of the acquired ultrasound data (Fig. 1) can reduce this problem. The scope of the algorithm, as indicated by these results, is approximately 15 mm with the deepest descent method currently used. The optimization criterion allows a correct identification of translational misalignments up to 40 mm.

Recapitulating the results of Figures 9 and 10, the average gray-value criterion can detect fairly large misalignments of up to 20° and 40 mm. The

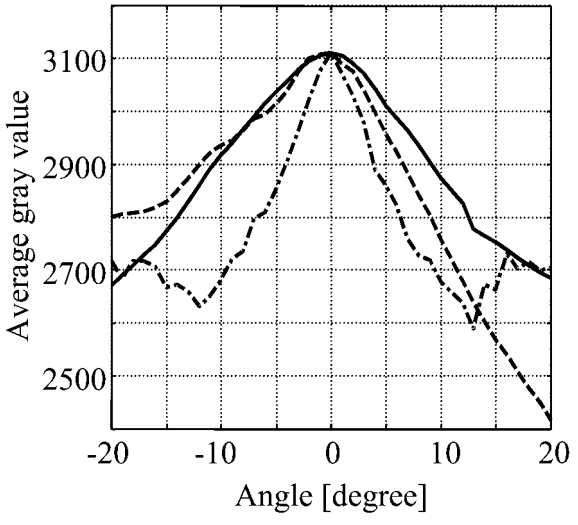

Fig. 9. The average gray value in dependence on rotational misalignments for rotations around the anterior–posterior (solid line), mediolateral (dashed line), and superior–inferior (dashed-dotted line) axes.

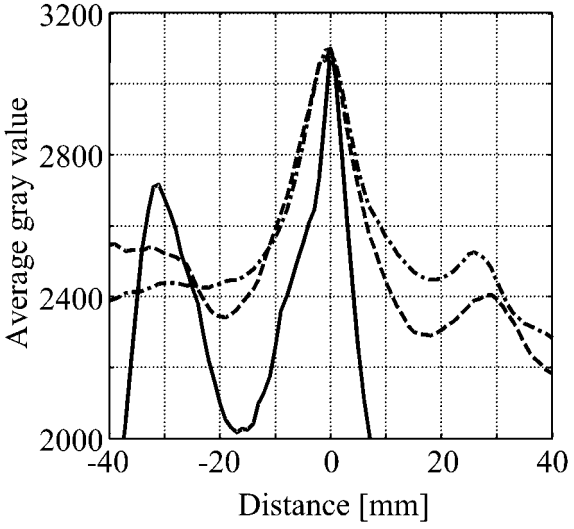

Fig. 10. The average gray value in dependence on translational misalignments for movements in the posterior (solid line, negative distance), anterior (solid line, positive distance), left (dashed line, negative distance), right (dashed line, positive distance), superior (dashed-dotted line, negative distance), and inferior (dashed-dotted line, positive distance) directions.

suboptimal deepest descent method employed reduces this scope to 12° and 15 mm.

CONCLUSION

We have presented a new method for the registration of preoperative CT datasets and intraoperative ultrasound data, which has many potential applications for navigated surgical interventions. The method is based on the extraction of bone surfaces from the preoperative dataset, while being aware of the characteristics and limitations of ultrasound imaging of bones.

Initial evaluations of the proposed algorithm have been done on an ex vivo preparation of a human lumbar spine. It was shown that the estimated surfaces are good predictors of the visibility of bone surfaces in ultrasound images, and that the algorithm is not sensitive with respect to the parameters for the surface extraction. The defined optimization criterion allows the determination of misalignments of up to 20° and several centimeters. Thus, a preregistration based on the scanning path of the transducer should be adequate. The repeatability and the computation time of the registration seem to be sufficient for many applications in navigated surgery. In the near future, we will apply these techniques to in vivo datasets to validate the clinical usefulness of the method, to further analyze its absolute position errors, and to integrate it into a prototype navigation tool for clinical evaluations.

ACKNOWLEDGMENTS

This work is an activity of the Ruhr Center of Competence for Medical Engineering (Kompetenzzentrum Medizintechnik Ruhr, KMR) Bochum, of which the respective institutions of the authors are members. The work is supported by the German Federal Ministry of Education and Research (Bundesministerium für Bildung und Forschung, Az.13N8079) and Siemens Medical Solutions, Siemens AG.

REFERENCES

1. Lavallée S. Registration for computer-integrated surgery: methodology, state of the art. In: Taylor RH, Lavallée S, Burdea GC, Mösges R, editors: Computer-Integrated Surgery: Technology and Clinical Applications. Cambridge, MA: MIT Press, 1995. p 77–97.
2. Maintz JBA, Viergever MA. A survey of medical image registration. Med Image Anal 1998;1:1–36.
3. Maurer CR, Fitzpatrick JM. A review of medical image registration. In: Maciunas RJ, editor: Interactive Image Guided Neurosurgery. Park Ridge, IL: American Association of Neurological Surgeons; 1993. p 17–44.
4. Maurer CR, Fitzpatrick JM, Galloway RL, Wang MY, Maciunas RJ, Allen GS. The accuracy of image guided neurosurgery using implantable fiducial markers. In: Lemke HU, Inamura K, Jaffe CC, Vannier MW, editors: Computer Assisted Radiology (CAR'95). Berlin: Springer-Verlag; 1995. p 1197–1202.
5. Fitzpatrick J, West JB, Maurer CR. Predicting error in rigid-body point-based registration. IEEE Trans Med Imaging 1999;5:694–702.
6. Audette MA, Ferrie FP, Peters TM. An algorithmic overview of surface registration techniques for medical imaging. Med Image Anal 2000;3:201–217.
7. Gering DT, Nabavi A, Kikinis R, Grimson WEL, Hata N, Everett P, Jolesz F, Wells WM. An integrated visualization system for surgical planning and guidance using image fusion and interventional imaging. In: Taylor C, Colchester A, editors: Proceedings of Second International Conference on Medical Image Computing and Computer-Assisted Intervention (MICCAI'99), Cambridge, UK, September 1999. Lecture Notes in Computer Science 1679. Berlin: Springer, 1999. p 809–819.
8. Zonneveld FW. Intra-operative CT: implementation of the Tomoscan M. Medicamundi 1998;1:6–11.
9. Carrat L, Tonetti J, Merloz P, Troccaz J. Percutaneous computer assisted iliosacral screwing: clinical validation. In: Delp SL, DiGioia AM, Jaramaz B, editors: Proceedings of Third International Conference on Medical Image Computing and Computer-Assisted Intervention (MICCAI 2000), Pittsburgh, PA, October 2000. Lecture Notes in Computer Science 1935. Berlin: Springer, 2000. p 1229–1237.
10. Maurer CR, Gaston RP, Hill DLG, Gleeson MJ, Taylor MG, Fenlon MR, Edwards PJ, Hawkes DJ. AcouStick: a tracked A-mode ultrasonography system for registration in image-guided surgery. In: Taylor C, Colchester A, editors: Proceedings of Second International Conference on Medical Image Computing and Computer-Assisted Intervention (MICCAI'99), Cambridge, UK, September 1999. Lecture Notes in Computer Science 1679. Berlin: Springer, 1999. p 953–962.
11. Muratore DM, Dawant BM, Galloway RL. Vertebral surface extraction from ultrasound images for technology-guided therapy. Proceedings of Medical Imaging. Bellingham, WA: SPIE, 1999. p. 1499–1510.
12. Amin DV, Kanade T, DiGioia AM, Jaramaz B, Nikou C, LaBarca RS. Ultrasound based registration of the pelvic bone surface for surgical navigation. First Annual Meeting of International Society for Computer Assisted Orthopaedic Surgery (CAOS-International), Davos, Switzerland, February 2001. p 36.
13. Kowal J, Amstutz CA, Nolte LP. On B-mode ultrasound based registration for computer assisted orthopaedic surgery. First Annual Meeting of International Society for Computer Assisted Orthopaedic Surgery (CAOS-International), Davos, Switzerland, February 2001. p 35.

14. Leotta DF, Detmer PR, Gilja OH, Jong JM, Martin RW, Primozich JF, Beach KW, Strandness DE. Three-dimensional ultrasound imaging using multiple magnetic tracking systems and miniature magnetic sensors. Proceedings of IEEE Ultrasonic Symposium. Piscataway, NJ: IEEE-UFFC, 1995. p 1415–1418.
15. Prager RW, Rohling RN, Gee AH, Bermann L. Rapid calibration for 3D freehand ultrasound. Ultrasound Med Biol 1998;6:855-869.
16. Muratore D, Galloway RL. Beam calibration without a phantom for creating a 3D freehand ultrasound system. Ultrasound Med Biol 2001;11:1557–1566.
17. Angelsen BAJ. Ultrasound Imaging. Norway: Emantec, 2000.
18. Sugano N, Sasama T, Nakajiama Y, Sato Y, Nishii T, Iida T, Nakagawa K, Ono K, Nishii T, Nishihara S, Tamura S, Yonenubu K, Ochi T. Effects of CT threshold value to make a surface bone model on accuracy of shape-based registration in a CT-based navigation system for hip surgery. In: Lemke HU, Vannier MW, Inamura K, Farman AG, Doi K, editors: Computer Assisted Radiology and Surgery. Proceedings of the 15th International Congress and Exhibition (CARS 2001), Berlin, June 2001. Amsterdam: Elsevier, 2001. p 306–311.